International Institute for
Applied Systems Analysis
Schlossplatz 1
A-2361 Laxenburg, Austria

Tel: +43 2236 807 342
Fax: +43 2236 71313
E-mail: publications@iiasa.ac.at
Web: www.iiasa.ac.at

Interim Report **IR-03-020**

A Comparison of the Classification of Vegetation Characteristics by Spectral Mixture Analysis and Standard Classifiers on Remotely Sensed Imagery within the Siberia Region

Su-Yin Tan (suyin@crsa.bu.edu)

Approved by

Sten Nilsson
Deputy Director and Leader, Forestry Project

16 May 2003

Contents

Abstract

As an alternative to the traditional method for inferring vegetation cover characteristics from satellite data by classifying each pixel into a specific land cover type based on predefined classification schemes, the Spectral Mixture Analysis (SMA) method is applied to images of the Siberia region. A linear mixture model was applied to determine proportional estimates of land cover for, (a) agriculture and floodplain soils, (b) broadleaf, and (c) conifer classes, in pixels of 30 m resolution Landsat data. In order to evaluate the SMA areal estimates, results were compared with ground truth data, as well as those estimates derived from more traditional image classification methods, including supervised and unsupervised classifiers. The findings of this study show that the SMA method offers a more sophisticated method of image classification, providing improved estimates of endmember values and subpixel areal estimates of vegetation cover classes than the traditional approach of using predefined classification schemes with discrete numbers of cover types. This technique enables the estimation of proportional land cover type in a single pixel and could potentially serve as a tool for deriving improved estimates of vegetation parameters that are necessary for modeling carbon processes.

Acknowledgments

I would like to express my thanks to Ian McCallum, Sten Nilsson and Anatoly Shvidenko of IIASA's Forestry (FOR) Project, for supervising this work and providing valuable comments and advice throughout the development of this research. I am also grateful to colleagues who are participating in the SIBERIA II study, as well as to other members of the FOR team who provided support and valuable advice. Special thanks are also due to Richard Kidd and Soeren Hese for providing useful comments. Finally, sincere thanks is extended to fellow participants in the Young Scientists Summer Program (YSSP) of 2002, all of whom made the summer program a most enjoyable and memorable experience.

About the Authors

Su-Yin Tan is currently pursuing a doctoral degree in environmental remote sensing and geographic information systems (GIS) at the Department of Geography at Boston University, USA. Her research interests include the application of remote sensing and GIS tools to natural resource management and environmental monitoring and modeling. She maintains a strong interest in issues relating to environmental change, sustainability, and conservation.

Su-Yin is originally from Canada and completed an undergraduate degree in Environmental Science at the University of Guelph, Ontario. Upon graduation, she accepted a Presidential University Graduate Fellowship to pursue postgraduate study at Boston University. She is currently a research assistant to a project funded by NASA, pertaining to the applications of machine learning and data mining for intelligent data understanding of high dimensional remotely sensed data.

Su-Yin was a participant in the 2002 Young Scientists Summer Program (YSSP), assigned to the Forestry (FOR) Project. Her research pertained to the classification of vegetation characteristics by spectral mixture analysis of remotely sensed imagery within the Siberia region. This project contributed towards the understanding of the measurement of required parameters for greenhouse gas modeling in the SIBERIA II study.

A Comparison of the Classification of Vegetation Characteristics by Spectral Mixture Analysis and Standard Classifiers on Remotely Sensed Imagery within the Siberia Region

Su-Yin Tan

1 Introduction

IIASA's Forestry (FOR) Project is using remote sensing and geographic information systems (GIS) technologies to create a set of tools to assist in producing and maintaining databases that are spatially and thematically suitable for conducting full carbon accounting. In line with this long-term goal, IIASA is collaborating in the SIBERIA II study, which is geared towards exploring multi-sensor concepts for greenhouse gas (GHG) accounting of Northern Eurasia. The overall objective of SIBERIA II is to demonstrate the viability of full carbon accounting (including various GHGs) on a regional basis using the environmental tools and systems available today and in the near future (Schmullius *et al*., 2002). The region under study lies within Northern Eurasia, approximately 300 million hectares in area and represents a significant part of the earth's boreal biome, thus playing a critical role in terms of global climate. A key objective of SIBERIA II is to make use of the developments made in European space technology and increased scientific expertise in remote sensing and processing of satellite images to produce more accurate quantitative data on the boreal biome. This information can then be used as intermediate products for vegetation and climate models for carbon cycle predictions and evaluation of future global change.

In general, remote sensing provides important coverage, mapping, and classification of land cover features, such as vegetation, soil, water, and forests. A chief use of remotely sensed data is to produce a classification map of the identifiable or meaningful features or classes of land cover types in a scene (Jasinski, 1996). As a result, the chief product is a thematic map with themes, such as land use, geology, and vegetation types. In the field of remote sensing, image classification is a process in which pixels or the basic units of an image are assigned to classes. By comparing pixels to one another and to those of known identity, it is possible to assemble groups of similar pixels into classes that match the informational categories of interest to users of remotely sensed data. Numerous methods of image classification exist and classification has formed an important part of not only remote sensing, but also of the fields of image analysis and pattern recognition. In some instances, the classification itself may form the object of the analysis and serve as the final product. In other instances, the classification may

form only an intermediate step in more elaborate analyses, such as land degradation studies, process studies, landscape modeling, coastal zone management, resource management, and other environmental monitoring applications. Therefore, image classification forms an important tool for examining digital images. Accordingly, the selection of which classification technique to employ can have a substantial effect on the results, whether the classification is used as a final project or as one of several analytical procedures applied to derive information from an image for further analyses.

The traditional method for inferring characteristics about vegetation cover from satellite data is to classify each pixel into a specific land cover type based on a predefined classification scheme. An alternative approach is to use a mixed pixel method or Spectral Mixing Analysis (SMA). This method recognizes that a single pixel is typically made up of a number of varied spectral types (i.e., soil, water, vegetation) (Atkinson *et al.*, 1997). The resulting land cover maps can be used in conservation and biodiversity assessments, land resource management, and extrapolation of results from more locally-based studies of the human dimensions of global change (Townshend *et al.*, 1994). In particular, applications of SMA for monitoring carbon sequestration has only begun to be developed and this technique offers a potentially useful tool in using remote sensing to measure biomass and other vegetation characteristics that can be used in biosphere–atmosphere models, global change studies, and other applications.

The objective of this research was to test the stability of a spectral mixture modeling method by applying the model to produce land cover maps of a study area within Northern Eurasia. Classification results from applying the spectral mixture model was assessed by comparison with those produced by more common classification techniques, such as by the maximum likelihood classifier. The SMA analysis was performed and evaluated, based on Landsat-7 data. Therefore, in line with the aims of the SIBERIA II study, this research was able to test an image processing technique that could potentially serve as a tool for deriving improved estimates of vegetation parameters that are essential for modeling carbon processes.

2 Background

Image classification is defined as the process of creating thematic maps from satellite imagery (DeFries, *et al*., 1999). The extraction of thematic information from remotely sensed images into the form of a thematic map is a key area of research into the applications of remote sensing data. By definition, a thematic map is an informational representation of an image, which conveys information regarding the spatial distribution of a particular theme (Campbell, 1996). Themes may be as diversified as their areas of interest. Examples of themes include soil, vegetation, water depth, and atmosphere.

The objective of image classification is to classify each pixel of an image into land cover categories. In the case of crisp or *hard classification*, each pixel is assigned to only one class. However, in fuzzy or *soft classification*, a pixel is associated with many land cover classes. In general, classification techniques may be categorized by the training process on which it is based (supervised or unsupervised) or on the basis of the underlying theoretical model (parametric or non-parametric).

The term *classifier* refers loosely to a computer program that implements a specific procedure for image classification. Many classification strategies have been devised over the years and from these alternatives, the analyst must select the classifier that will best serve the task or application at hand. The optimal classifier depends on the situation at hand, since characteristics of each image and the circumstances for each study vary greatly. Therefore, it is imperative that the spatial analyst understands the alternative strategies available for image classification in order to select the most appropriate classifier for a specific task. For this reason, different digital image classifiers will be reviewed and evaluated before proceeding to describe the technique of spectral mixture analysis.

2.1 Digital Image Classifiers

Several classification algorithms (classifiers) have been developed and categorized as either *supervised* or *unsupervised* approaches, or based on *parametric* or *non-parametric* models. For example, the Maximum Likelihood Classifier (MLC) is a supervised parametric algorithm, whereas k-means clustering is considered to be an unsupervised parametric algorithm. Both types of classifiers are commonly used in the classification of remotely sensed imagery.

2.1.1 Supervised Classification

Supervised classification procedures tend to require considerable interaction with the analyst, who must guide the classification by identifying areas on the image that are known to belong to each category. These areas are referred to as training sites. The training sites or samples of known identity are then used to classify pixels of unknown identity. Examples of supervised classification methods include parallelepiped, maximum likelihood, minimum distance, and Mahalanobis distance classifiers.

In general, supervised classification involves three distinct stages of training, allocation, and testing. Training involves the identification of the training sites to be used by the classifier and such pixels of known class membership are usually gathered from reference data sources including ground truth data, existing maps, and aerial photographs. These training sites are used to derive various statistics, such as the mean, variance, divergence measures, and covariances of spectral properties that typify each informational category or land cover class to be classified. This information is input into the second stage of the classification. In the allocation phase, the pixels of the image are allocated to the class with which they show the greatest similarity based on the derived statistics. In the final stage, the overall accuracy of the classification procedure is determined. This is accomplished by selecting a sample or group of testing pixels and comparing their class identities on both the classified image and the reference data. The pixels of agreement and disagreement for each testing sample are represented in the form of an error matrix, which can be used to evaluate the classification accuracy.

A variety of methods have been devised to implement the basic approach of supervised classification. All of these methods use information derived from the selected training data as a means of classifying uncategorized pixels. The method of *parallelepiped classification*, or sometimes referred to as box decision rule or level slice procedures, is

based on the ranges of values within the training data to define decision boundaries within a multidimensional data space (Colwell, 1983). The spectral values of unclassified pixels are projected into data space and those falling within the regions defined by the training data are assigned to the appropriate categories. The dimensions of the parallelepiped are usually defined based upon a standard deviation threshold from the mean of each selected class. Although this procedure has the advantages of accuracy, directness and simplicity, the disadvantages of this method are also obvious. For example, spectral regions for informational categories may intersect or the training data may not encompass the complete range of values to be classified in an image.

Another commonly used classifier is *maximum likelihood classification*. This method assumes that the statistics for each class in each band are normally distributed and calculates the probability that a given pixel belongs to a specific class (Settle and Briggs, 1987). All pixels are classified or assigned to a specific category, unless a probability threshold is specified. Therefore, each pixel is assigned to the class to which it has the highest probability (i.e., the "maximum likelihood") of belonging.

The *minimum distance classification* differs in that it uses the mean vectors of each region of interest and calculates the Euclidean distance from each unknown pixel to the mean vector for each class. All pixels are classified to the closest region of interest class unless the user specifies standard deviation or distance thresholds, in which case some pixels may be unclassified if they do not meet the selected criteria.

The *Mahalanobis distance classification* is a direction sensitive distance classifier that uses statistics for evaluating each class (Schowengerdt, 1997). Although this classifier is similar to the maximum likelihood classifier, it assumes that all class covariances are equal. As a result, this approach is a faster method of classification. More specifically, all pixels are classified to the closest region of interest class unless the user specifies a distance threshold, in which case some pixels may be unclassified if they do not meet the threshold.

Supervised classification methods have many advantages, relative to unsupervised classification. Firstly, the analyst has control of a set, selected menu of informational categories tailored to a specific purpose and geographic region (Campbell, 1996). This control is essential when the specific task is to compare one classification with another of the same scene at different dates, or if the classification must be compatible with those of adjacent regions. Secondly, supervised classification is associated with specific areas of known identity as a result of selecting training areas. As opposed to unsupervised classification methods, the analyst is not required to manually match spectral categories on the final map with the informational categories of interest. Finally, serious classification errors are detectable by examining training data to determine whether they have been correctly classified. On the other hand, supervised classification also has numerous disadvantages. In effect, the analyst imposes a classification structure upon the data based on predefined classes instead of finding "natural" classes in an image. Furthermore, the defined classes may not match the natural classes that may exist in the data. In supervised classification, training sites and classes are based primarily on information categories and only secondarily on spectral properties. Another source of error is in the selection of training data, since these samples of pixels may not be representative of conditions encountered throughout the

image. Moreover, supervised classification may not be able to recognize and represent special or unique categories not represented in the training data, possibly due to the small areas they occupy on the image or simply because they are not known to the analyst. Finally, a priori class training can often be a time-consuming and tedious process. For example, matching delineated training sites on maps and aerial photographs to the image to be classified may be problematic, especially if the area to be classified is large, complex, or inaccessible. Nevertheless, previous experience has shown that supervised classification methods typically produce better maps than unsupervised classifications, provided that good training data are available (Schowengerdt, 1997). The key factor in a supervised classification is the ability to identify a set of pixels that accurately represents the spectral variation present within each informational region.

2.1.2 Unsupervised Classification

As stated earlier, unsupervised classification involves the process of automatically segmenting an image into spectral classes based on the natural groupings found within the data set. The objective is to group multiband spectral response patterns into clusters that are statistically separable. In unsupervised classification, any individual pixel is compared to each discrete cluster to see which one it is closest to, in terms of spectral value.

Typically, an unsupervised classification begins with the analyst specifying minimum and maximum numbers of categories to be separated by the classification algorithm (Colwell, 1983). A set of pixels is arbitrarily selected as cluster centers. The classification algorithm determines the distances between pixels and initial estimates of cluster centers are formed. The statistical center or class centroid is determined for each class in order to define the exact center of the group. In the next step, all the remaining pixels in an image are assigned to the nearest class centroid. The final step involves testing the distinctiveness of the identified classes.

The two most frequently used grouping algorithms are the K-means and the ISODATA clustering algorithms. These two statistical routines for grouping similar pixels together are iterative procedures. In general, both algorithms assign first an arbitrary initial cluster vector, then each pixel is classified to the closest cluster. The new cluster mean vectors are calculated based on all the pixels in one cluster. This procedure is repeated until the change between the iteration is small. The change between iterations can be specified in several different ways, either by measuring the distances the mean cluster vector have changed from one iteration to another, or by the percentage of pixels that have changed between iterations.

The ISODATA algorithm has some refinements to the general unsupervised classification procedure by the splitting and merging of clusters (Campbell, 1996). It can also be considered a variation on minimum distance methods. Clusters are merged if either the number of members (pixels) in a cluster is less than a certain threshold or if the centers of two clusters are closer than a certain threshold. Clusters are split into two different clusters if the cluster standard deviation exceeds a predefined value and the number of members (pixels) is twice the threshold for the minimum number of

members. The ISODATA and k-means algorithms are similar, except that the ISODATA algorithm allows for a different number of clusters while the k-means assumes that the number of clusters is known *a priori*. It is also true that the ISODATA algorithm has some resemblance to supervised classification in that initial estimates of class means can be derived from available training data. Therefore, this algorithm is sometimes considered to be a hybrid classifier rather than a clear example of either supervised or unsupervised approaches.

The k-means algorithm is a common clustering method, which seeks to minimize the within cluster variability. The first step of the algorithm involves specifying an initial mean vector (seed or attractor) for each of the k clusters. Each pixel of the training set is then assigned to the class whose mean vector is closest to the pixel vector, forming the first set of decision boundaries. The procedure is iterative, since a new set of cluster mean vectors is then calculated from this classification, and the pixels are reassigned accordingly. In each iteration, the k-means will tend to gravitate towards concentrations of data within their currently-assigned region of feature space. This procedure is repeated until there is no significant change in pixel assignments from one iteration to the next.

Advantages of unsupervised classification can be summarized into three key points. Firstly, no extensive prior knowledge of the region of interest is required. Compared to supervised classification, where detailed knowledge of the area was required to select training sites, unsupervised classification does not require detailed prior knowledge. The only stage when knowledge of the region is required is when interpreting the meaning of the results produced by the classification process. Secondly, the opportunity for human error is minimized. Many of the detailed decisions required for supervised classification are not required for unsupervised classification, so the analyst is presented with less opportunity for error. Finally, unique classes are recognized as distinct units in unsupervised classification. Such classes, perhaps of very small areal extent, may remain unrecognized in the process of supervised classification and could inadvertently be incorporated into other classes, generating error and imprecision throughout the entire classification.

On the other hand, disadvantages and limitations arise primarily from a reliance on finding “natural” groupings in the image and difficulties in matching these groups to the information categories of interest. Since unsupervised classification identifies spectrally homogeneous classes within the data, such classes do not necessarily correspond to the informational categories that are of interest to the analyst. There is seldom a simple one-to-one correspondence between matching the spectral class with an informational class. Furthermore, the analyst has limited control over the menu of classes and identities. In the situation where an analyst must compare classifications for different dates or adjacent regions, the use of unsupervised classification techniques may be unsatisfactory, since a specific menu of informational classes cannot be generated.

In summary, unsupervised classification tends to be too much of a generalization in that the spectral clusters only roughly match some of the actual classes. Its value is mainly as a guide to the spectral content of a scene and can be used to aid in making a preliminary interpretation prior to conducting a supervised classification procedure.

2.2 Spectral Mixture Analysis

Spectral Mixture Analysis (SMA) is an alternative to the traditional approach of using predefined classification schemes with discrete numbers of cover types to describe the geographic distribution of land cover (DeFries *et al.*, 2000). In effect, SMA is a technique used to measure the percentage of spectra for each land cover type in a single pixel. In previous studies, SMA has been successfully used to classify successional forest types and forest types of varying carbon sink strengths (Settle and Drake, 1993). Using SMA as an alternative to traditional classifiers has been recommended by previous studies, as it takes into consideration changing biological variables (DeFries *et al.*, 2000). The SMA process enables the classification of different forest types, although it still has difficulties in classifying species type and age class with confidence. Using ground-based data is especially useful with respect to increasing the accuracy of such classifications.

SMA is based on the assumption that the reflectance spectrum derived from an air- or spaceborne sensor can be deconvolved into a linear mixture of the spectra of different ground components, frequently referred to as spectral endmembers (Bateson and Curtiss, 1996). Various methods of SMA have been developed to improve the classification of mixed pixels and to detect and identify subpixel components and their proportions. Most of the techniques have employed a linear mixing approach (Foody and Cox, 1994). Linear mixing refers to additive combinations of several diverse materials that occur in patterns too fine to be resolved by the sensors.

The linear mixture model assumes that as long as the radiation from component patches remains separate until it reaches the sensor, it is possible to estimate proportions of component surfaces from the observed pixel brightness.

In effect, with a known number of endmembers and known spectra of each pure component, the observed pixel value in any spectral band is modeled by the linear combination of the spectral response of component within the pixel. The linear mixture model can be mathematically described as a linear vector-matrix equation,

$$DN_i = \sum_{j=1}^{n} (R_{ij} \times F_j) + E_i$$

$i = 1,\ldots,m$ (number of bands);
$j = 1,\ldots,n$ (number of endmembers);
DN_i = spectral reflectance of the ith spectral band of a pixel;
R_{ij} = known spectral reflectance of the jth component;
F_j = the fraction coefficient of the jth component within the pixel;
E_i = error for the ith spectral band.

The error terms account for the unmodeled reflectance and represent the unknown noise of observations. The assumption of this relationship is that an exhaustive set of endmembers or classes is defined, so that,

$$\sum_{j=1}^{n} F_j = 1$$

at each pixel. This assumption poses a problem, since one can never be sure that a sufficient number of endmembers has been defined for a given set of data.

Nevertheless, SMA is a useful method of image classification; particularly for defining proportions of land cover types in pixels for coarser resolution satellite imagery. Whereas conventional image classification matches pixels to broad classes of features, SMA attempts to identify surfaces from their spectral data much more precisely than was previously possible. In effect, this method of classification attempts to classify impure pixels and to quantify the proportion of each land cover type comprising a pixel. As a result, more precise estimates of vegetation characteristics, such as quantifying aboveground biomass, are made possible.

3 Study Area

Under the broad framework of SIBERIA II, the region under study lies within Northern Eurasia, representing a significant part of the earth's boreal biome and playing a critical role in the global climate. The project area location of SIBERIA II is shown in Figure 1, a region spanning from 52 to 77 degrees north latitude and 80 to 119 degrees east longitude. This territory represents a region of significant size (3,000,000 km^2) for image classification purposes, which is one of the preliminary steps for regional GHG accounting to derive variables such as aboveground biomass, forest cover area, and forest composition.

A small sample of the broad region of interest was subset for preliminary testing purposes. This would result in a smaller sample of image pixels that would offer the advantage of ease in processing and would be inexpensive with respect to time and costs. The subset area should also be representative of the forest area and vegetation types, as well as large enough to test a variety of classification techniques.

In accordance to this rationale, this study was conducted on the Shestak test area (103.5 E, 56.7 N), which is situated in the center of the Irkutsk Oblast, in the Angara river basin as shown in Figure 2. The Angara basin is dominated by mixed coniferous and pine forests located at the merging of the Birjusa and Chuna rivers (Sakhatsky *et al.*, 2002). The terrain is hilly and pine forests cover approximately a quarter of the area. The mixed coniferous forests vegetation type is typical of flat watersheds in the south of this region and of higher altitudes of landscapes between the Taseeva and Angara rivers.

The vegetation types occurring in the study area were typical of Siberian forest cover. As aforementioned, the forest composition of the study area was dominated by pine forests, which occupied approximately 45% of the forest area (Sakhatsky *et al.*, 2002). Smaller areas near the base of slopes and on sandy podzol soils were characterized by growth of pine forest. Spruce forests occurred at lower elevations, occupying about 12% of the area. A smaller area of spruce forests was present on drained watersheds and slopes. Fir forests tended to dominate drained and flat watershed areas, as well as humidified slopes on the western part of the region. Aspen forests prevailed mainly at the bottom of slopes and flat watersheds, usually existing as the precursor or initial stage of regeneration of fir or pine forests. Cedar forests of wet slopes were typical for small sites in areas of low relief. Larch forests tended to cover an insignificant area of the forest and were usually restricted to places with frozen ground. In the later stages of regeneration, birch forests were found in the western half of the region and occupied less than a quarter of the total forest area.

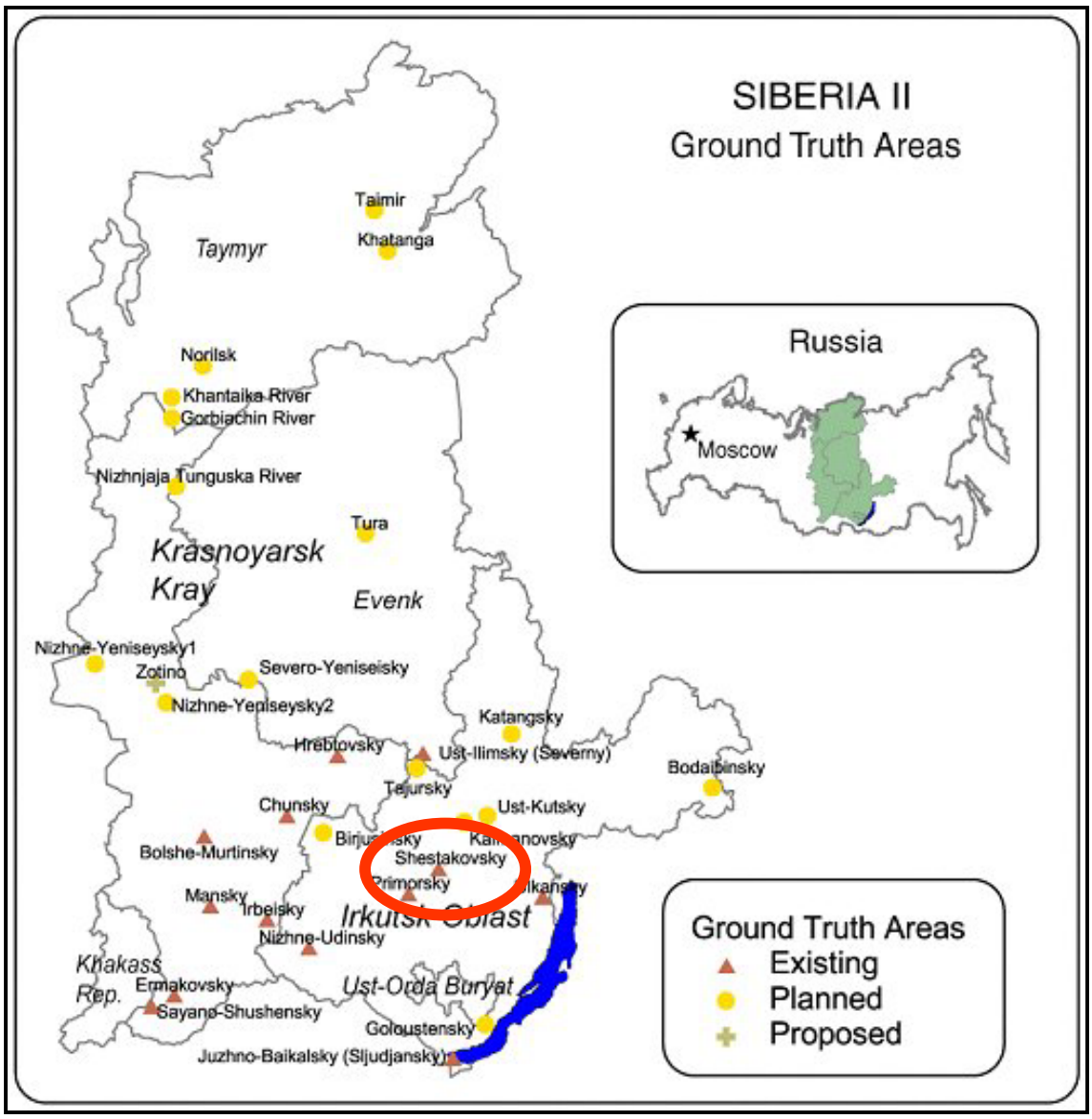

Figure 1: Siberia II research territory located in Northern Eurasia, with Shestak test area (circled used in this study.

The particular test area was selected, since it offered a variety of land cover types for the purposes of image classification, detailed ground truth data were readily accessible, and a cloud-free satellite image was available. Furthermore, the mixed forest composition of this area provided an interesting scenario for the application of SMA methods of land cover classification, since different tree species and vegetation types comprising an area exhibits different spectral characteristics. In summary, the diversity of vegetation and land cover patterns made the Shestak study site an ideal sample of the broader Siberian forest region for testing a variety of vegetation mapping methods and implementing the SMA technique.

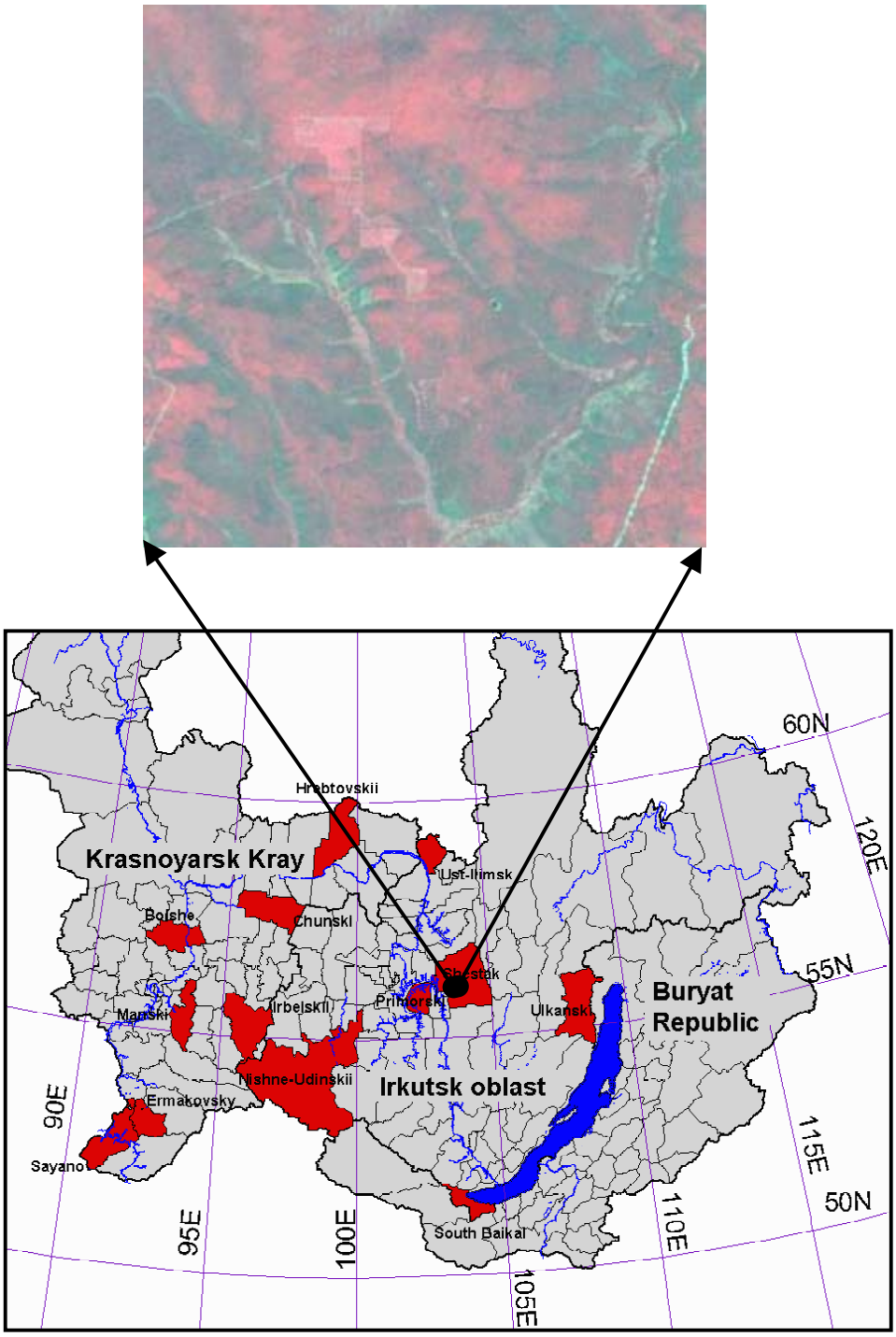

Figure 2: Research territory showing IIASA test areas (shaded red), containing test sites with forest inventory in GIS format. The focus of this study was on a test site within the Shestak test area. The corresponding Landsat scene in 30 m resolution is also shown with the delineation of the Shestak test area boundary.

4 Software and Data Sources

This study considered one test area (Shestak) containing forest ground truth data and Landsat-7 coverage. Ground truth data were encoded as forest inventory polygons and attributes in GIS format (i.e., species composition, forest density, land-cover/land-use). Landsat-7 ETM+ was available at 30 m resolution with six spectral bands (excluding the panchromatic band and thermal band) (1: .45–.52 micrometers (μm); 2: .53–.61 μm; 3: .63–.69 μm; 4: .78–.90 μm; 5: 1.55–1.75 μm; 6: 2.09–2.35 μm).

The Landsat-7 ETM+ scene used in this study was acquired on 8 August 2000 from path 135, row 21. The scene was a level 1G product and was radiometrically and geometrically corrected (systematic). The resulting product is free from distortions related to the sensor (e.g., jitter, view angle effect), satellite (e.g., attitude deviations from nominal), and earth (e.g., rotation, curvature). Residual error in the systematic L1G product is less than 250 meters (1 sigma) in flat areas at sea level. The systematic L1G correction process does not employ ground control or relief models to attain absolute geodetic accuracy. Cloud coverage over the area of interest was negligible.

The quality of the Landsat images was relatively good and used for deriving the training sites for supervised classification. The particular Landsat scene selected of the Shestak test area was selected for a number of reasons, including availability of near cloud-free data, availability of ancillary data to interpret the scene, and location in an area where significant land cover changes since the time of acquisition was not expected. Although some land use activity was present, such as agricultural areas in the center of the image, this contributed to the diversity of vegetation cover types present in the image and enabled testing of the ability of the classification algorithm to discriminate amongst a variety of land cover types as well as forest tree types.

The emphasis in this study was placed on the analysis of Landsat satellite imagery, because it is higher resolution data (i.e., relative to SPOT vegetation data) and the most commonly used imagery when referring to previous studies that employed classification and SMA methodology (Shimabukuro and Smith, 1991). Utilization of Landsat imagery facilitated the testing of a variety of classifiers and SMA techniques for the purposes this study and such techniques can potentially be applied to other types of coarse to fine resolution satellite data.

In this study, public domain image processing software, commercial image processing software, and GIS software were used to carry out the analysis. The Image Processing Workbench (IPW) was used for most image processing purposes. IPW is a UNIX-based image processing system, which includes several UNIX filter programs that can be pipe-lined together to form complex image processing algorithms. Due to the programming capabilities of IPW and the level of control that the user can exert over the manipulation of images, it offered an efficient method for processing the types of image data that were available to this study. Another advantage of using IPW software for this analysis was the ease of adding programs to the existing SMA package by composing c shell scripts.

The commercial image processing software, ERDAS Imagine 8.4 (ERDAS, 1997) was also used in this study. This software was used mainly for importing data,

preprocessing purposes, and executing the unsupervised classification. Data processing and analysis were also executed in an ArcView and Arc/Info GIS environment, which was used to organize, process, and display the data layers of available ground truth data for the Shestak test area. All operations were carried out either in a Windows environment or on a Sun Sparc 2 workstation. Other software packages were primarily used for statistical analyses, such as Microsoft Excel, version 9.0.

5 Methodology

This study considered one test site from the Shestak area containing forest inventory polygons and attributes in GIS format and complete Landsat-7 coverage for one season. By comparing the ground truth data with the satellite images by performing a simple overlay in ArcView, further geometric correction of the images were not deemed to be necessary. This judgment was based on the examination of the alignment of forest stand boundaries, intersections of roads, boundaries of agricultural areas, and river tributaries between the satellite image and ground truth layer. Although more accurate georeferencing could have been performed, this was not applied given the time constraints and the fact that the image was considered only as a "test site" for investigating classification methodology. Therefore, geometric accuracy was not a central issue in this study and additional georeferencing was not necessary, although offset forest stand boundaries could potentially produce some error with respect to proportional cover estimations. Furthermore, since the image was cloud-free, no atmospheric corrections were applied at this stage.

A window of 312 × 359 pixels was clipped from the input Landsat image and used for the purposes of classification analyses in this study. This area represented in the GIS inventory is shown in Figure 3.

5.1 Spectral Mixture Analysis

The procedure used in this study was based on a linear mixture model to derive continuous fields of, (a) broadleaves (hardwoods), (b) conifers (softwoods), and (c) agriculture and floodplain soils (other vegetation and land cover types). As previously mentioned, the linear mixture model is based on the assumption that the reflectance at a pixel is the sum of the reflectances of each component within the pixel weighted by the respective proportional covers. It should be noted that improvements on this simple linear model have been proposed in the literature. For example, Roberts *et al*. (1998) tested an approach that allowed the number and types of endmembers to vary on a per pixel basis. Bosdiagianni *et al*. (1997) proposed to augment the model to include higher order moments that describe the distribution of the endmember values about the mean. The application of artificial neural networks (ANNs) to estimate the proportions of each component has also been suggested; since this nonparametric method does not make the underlying assumption that the reflectance is a linear sum of the reflectances from each component (Foody *et al.*, 1997). However, for the purposes of this study, the SMA procedure was restricted to the simple linear mixture model as a basic form of analysis and estimation of continuous fields from satellite data.

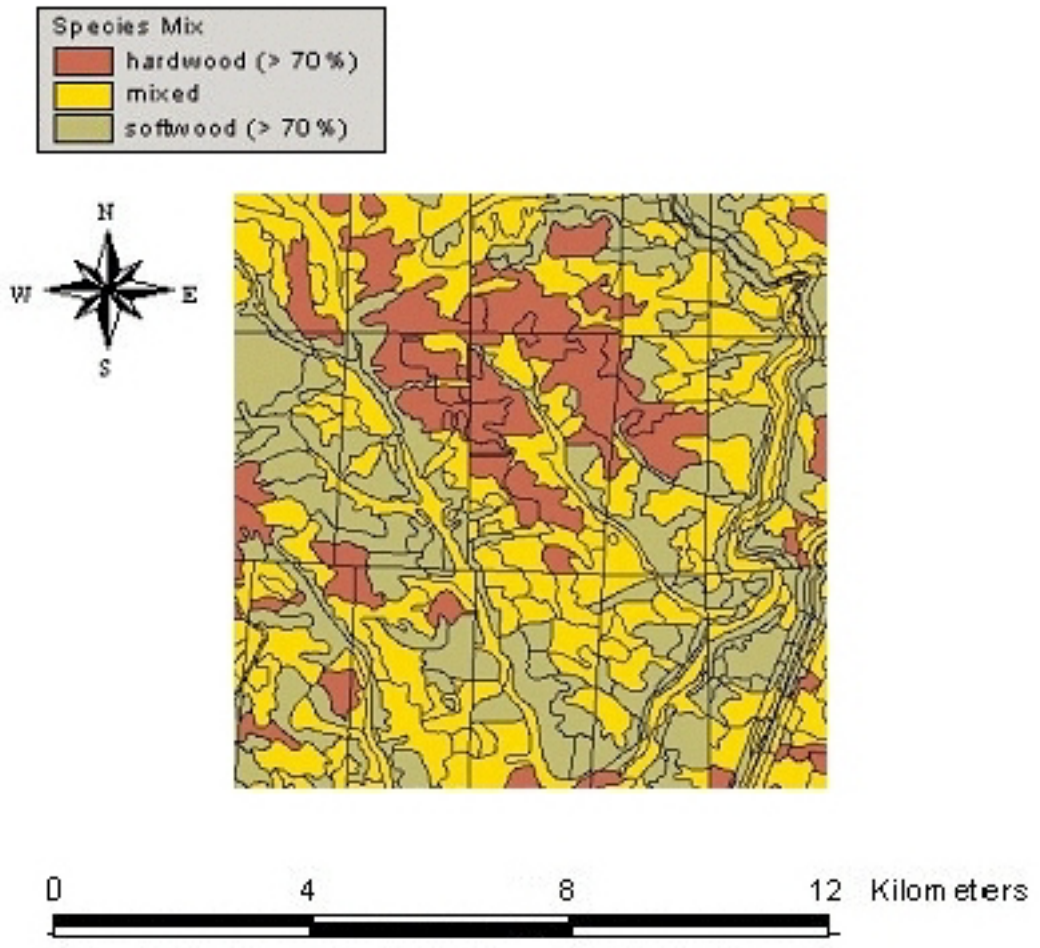

Figure 3: Forest regions within the Shestak research area from ground truth data shown in an ArcView GIS layer. Forest composition is shown in three classes of hardwood, mixed forest, and softwood species mix.

The SMA was performed on the partial Landsat scene of the selected Shestak test site. The procedure for deriving the continuous fields is described by DeFries *et al*. (1999) and involved the following steps (Figure 4).

(1) Field data consisting of a series of test stands was obtained in the form of a region map separating the pixels of the image and identifying the pixels belonging to each forest test stand. Field data also included the proportions of agriculture and floodplain soils, broadleaves, and conifers for each stand.

The region-based analysis of forest structure was a key characteristic of the SMA technique described here. During this early stage of the mapping process, the image was divided into a large number of small patches representing individual forest stands. The resulting region map existed as an IPW image in which all pixels belonging to a given region had the same pixel value. Due to the large number of regions in most images, region maps generally contain two bytes per pixel. The

purpose of the region map was to define related sets of pixels, or regions, associated with the Landsat image layer (Woodcock *et al.*, 1993).

Forest stand boundary delineation was achieved by overlaying the ground truth data in GIS format over the subset Landsat scene. The region map was generated by using the region tool in IPW that enabled the user to manually define test stand boundaries. Since boundaries were drawn manually and geometric correction was not performed on the image, human error along with mismatch between the field data layer and satellite image may have produced slight inaccuracies in forest stand delineation. It was expected that the misidentification of pixels to their respective forest stands would cause some error in estimating the proportions of each land cover type in the subpixel classification analysis. However, this error was expected to have a minimal effect, since most forest stand boundaries were in close agreement and there was not a high degree of land cover heterogeneity or variability in the selected scene.

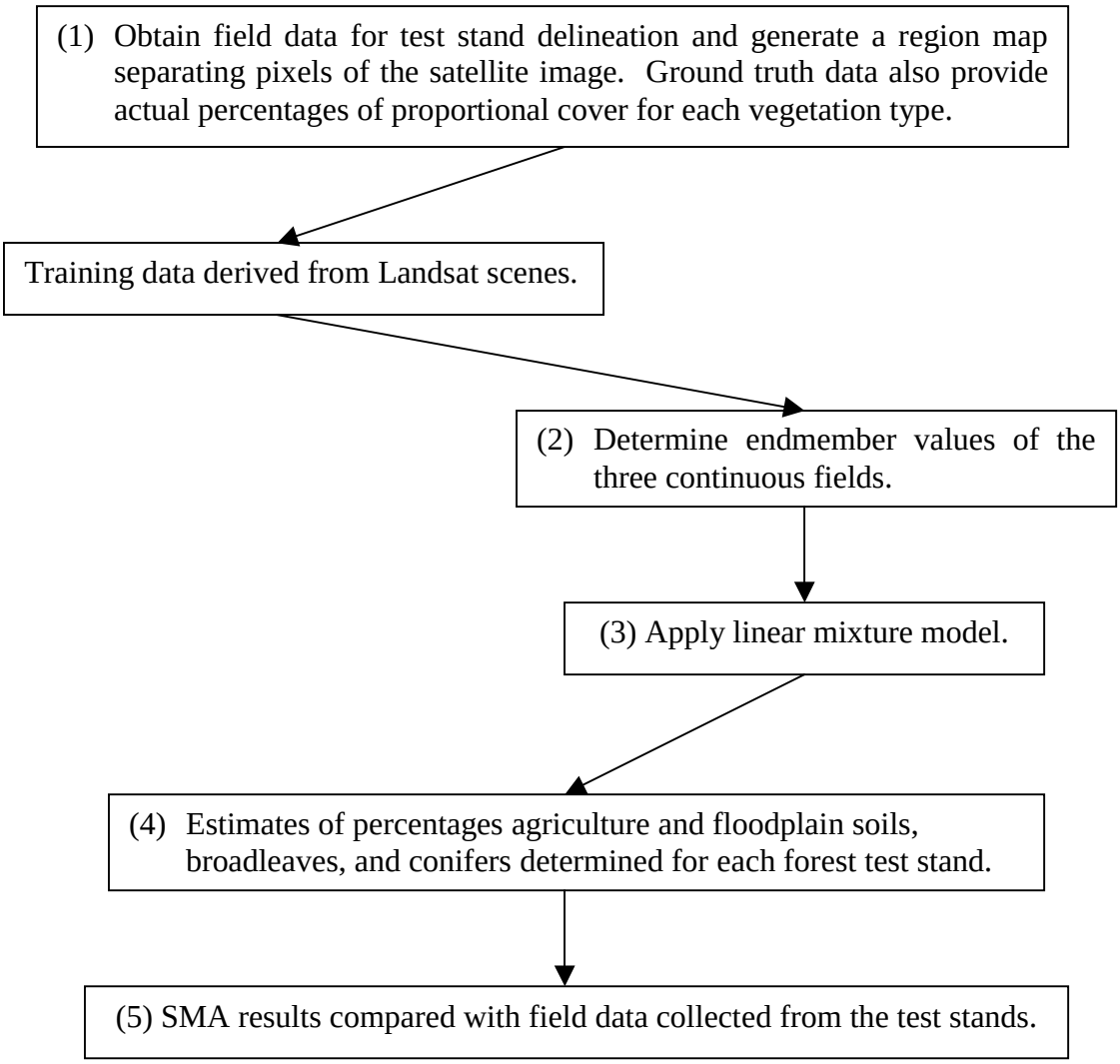

Figure 4: Procedure used in this study to derive continuous fields.

(2) Endmember values of the three continuous fields were determined based on the selected training data from the Landsat scene.

An endmember is defined as a pure material that is present or assumed to be present within an imaged scene (Moody, 1998). Examples would include asphalt, grass, water, etc. Endmembers may be very general (i.e., grass) or very specific (i.e., healthy grass, stressed grass, etc.) depending on the application. In this study, the purpose of performing an SMA analysis was to map different types of vegetation and land cover. Three broad classes of endmembers were selected, namely agriculture and floodplain soil, broadleaves, and conifers.

In general, accurate estimations of endmember values for each component in an SMA is essential in order to successfully apply the linear mixture model. Several approaches are available, including values obtained from field or laboratory measurements (Adams *et al.*, 1995), manual selection of endmembers based on principal components analysis (Bateson and Curtiss, 1996), and deconvolution of the mixture modeling equation to solve for the endmember values when the fractional cover is known (Oleson *et al.*, 1995; Asner *et al.*, 1997).

Since fractional cover data were not available and spectral field data could not be collected within the given time frame, training data were used to determine endmember values. Training sites were selected for each endmember, as shown in Figure 5. The pixel area estimate and percent of image area for each training site are shown in Table 1.

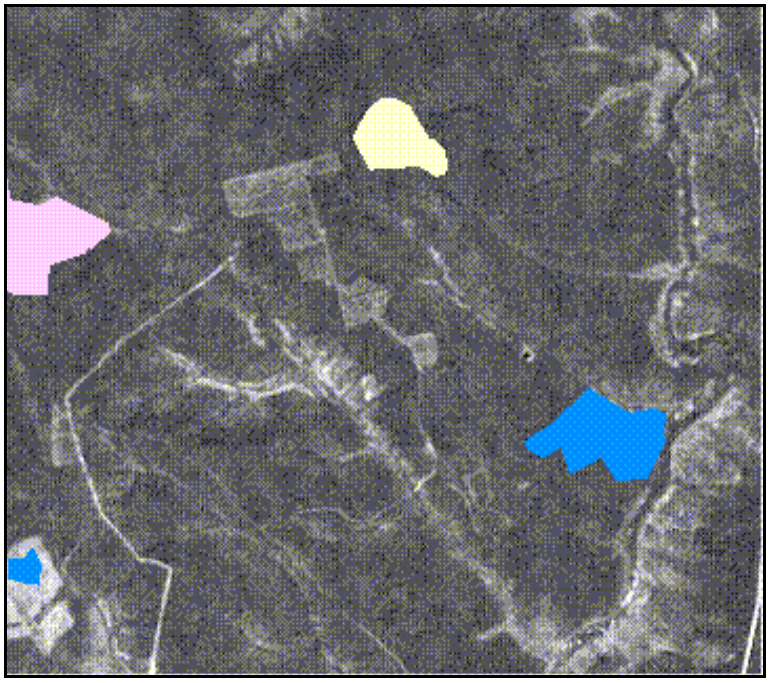

Figure 5: Training areas for determining endmember values of continuous fields, (a) agriculture and floodplain (left blue region), (b) broadleaf forest (yellow region), and (c) conifer forest (pink and right blue regions).

Table 1: Pixel areas and image proportions of training areas used for SMA and supervised classification.

DN	Pixels	Percentage	Cumulative Percentage
0	107551	96.02	96.02
1	1908	1.7	97.72
2	1054	0.94	98.66
3	1495	1.33	100

(3) The linear mixture model was applied. With three endmembers or continuous fields to be estimated for each pixel of a 6-band Landsat image, the mixture model becomes:

$$
\begin{aligned}
DN = \quad & [(R_{a1} \times F_a) + (R_{b1} \times F_b) + (R_{c1} \times F_c)] + \\
& [(R_{a2} \times F_a) + (R_{b2} \times F_b) + (R_{c2} \times F_c)] + \\
& [(R_{a3} \times F_a) + (R_{b3} \times F_b) + (R_{c3} \times F_c)] + \\
& [(R_{a4} \times F_a) + (R_{b4} \times F_b) + (R_{c4} \times F_c)] + \\
& [(R_{a5} \times F_a) + (R_{b5} \times F_b) + (R_{c5} \times F_c)] + \\
& [(R_{a6} \times F_a) + (R_{b6} \times F_b) + (R_{c6} \times F_c)] \\
& \quad a \qquad\quad b \qquad\quad c
\end{aligned}
\qquad \Big\downarrow \text{ 6 bands}
$$

where DN is the spectral reflectance of a pixel in the Landsat 6-band composite image, R_{ij} is the known spectral reflectance or endmember values for agricultural and floodplain soils, broadleaf, and conifer classes. The six bands of the Landsat scene were represented by the parameter *i* and each of the three endmembers was represented by factor *j*. F_j was the fraction coefficient of the jth component within the pixel or the fractional cover for agricultural and floodplain soils, broadleaves, and conifers.

The technical procedure involved determining the mean spectral reflectance values for each band of the Landsat composite image by using an image multivariate statistics program (i.e., mstats IPW program). By computing the basic multivariate statistics for the multiband satellite image, the mean pixel values, variances, and interband covariances were determined for each input band. The next step involved formatting the endmember values into a particular format for use in the SMA program, by using an interactive program for creating individual ascii files for each endmember. These files consisted of a line of endmember values for each spectral band in the corresponding image, containing six values in total. In order to compare endmember values among Landsat bands, the endmember files were plotted as spectra.

The spectral mixture model was applied by means of an SMA program in IPW. By default, a modified Gram-Schmidt method was used to invert the endmember matrix that was created. Since the fraction images were required to sum to one, coefficients were computed for n-1 endmembers. The final fraction image was then computed by means of subtraction.

(4) Estimates of percentages for agriculture and floodplain soils, broadleaves, and conifers were determined for each forest test stand.

The output of the SMA program consisted of fraction images (named with the endmember name with .fr extension). One fraction image was produced for each of the three endmembers. Such images or mixture maps contain the percent abundance or relative fraction of a specific material or endmember at each pixel location of the Landsat scene. Such image maps are usually generated as a set of mixture maps for a defined set of scene materials or endmembers. Ideally, the algorithms that generate mixture maps constrain the individual material fractions to the range of 0.0 to 1.0 and the fractions for a single pixel total to 1.0.

By default, the SMA program rescaled the output fraction images to digital number (DN) integers from 0 to 255, in order for each fractional image to be presented in an intuitive manner. The default range for fractional values was –1.0 to 1.55. Fractions less than –1.0 and greater than 1.55 were scaled to 0 and 255, respectively. This scaling was chosen for three main reasons. Firstly, this scaling increased the interpretability of each fractional image, as used by the original SMA implementation from the University of Washington (Quarmby *et al.*, 1992). Secondly, fractions outside the above range are usually meaningless. Finally, the precision of the input data does not justify using more than one byte for the output data.

In order to compare the resulting proportional estimates of each continuous field from each forest test stand with the collected field data, the first step involved converting the output from the SMA program to the percent covers of the different endmembers. However, the fractional files contain the estimates of the fractional coverage associated with each endmember and the values between 0 and 100 could be interpreted as percentages for that particular endmember. Since the SMA program was implemented as an unconstrained version, with no constraints on the values of the fraction images, not all fractional values were between 0 and 100, with some values below or higher than 100. In this case, values over 100 were considered outside the range of the endmembers and were stretched to 100. For example, areas such as water received values above 100 for the conifer class, since they were outside the range of the means from the three endmembers.

Since each endmember was evaluated separately and proportional cover estimates were determined independently, these values did not obey the constraint of the model that limits the sum of all fractions to a value of 1.0 in each pixel. Therefore, each fractional value was rescaled to result in 100 percent cover for each pixel by dividing the total sum of the fractions by 100 and in turn, dividing each fraction estimate by this factor. The re-scaling due to the sum-to-one constraint assumes that all endmembers in the image are known and each pixel is comprised only of the identified land cover types. This condition of identifiability of the composition of mixtures is one of the basic assumptions made by the linear mixture model for the SMA.

(5) The SMA results were compared with the field data collected from the test stands.

In order to compare the results of the SMA to the available land cover data set from the ground truth information, look-up tables were derived from each fraction map and placed in an ascii file. The ground truth data of actual proportions of each endmember were appended to the file for ease of comparison.

5.2 Supervised Classification

In order to evaluate classification results of the SMA, the image was first classified by a traditional supervised classification method, namely the Maximum Likelihood classifier.

In order to make results comparable to the SMA, the same informational categories or land cover types were used to classify the data. The same training sites digitized for the SMA were also used. The training sites were assumed to represent pixels of known identity and covered rather homogeneous regions of land cover. Training sites were then linearly stretched into their respective classes.

Supervised image classification began with computing statistics for the user-selected training sites of land cover classes and the results of the statistical summary were used to classify the image. The *mstats* IPW program was used to compute basic multivariate statistics (per band means, variances and interband covariance) for the input image. The statistics file that was generated was then input into a bayes algorithm to classify the image. This procedure constituted the Bayesian Maximum Likelihood method of image classification. This is the most common supervised classification method used with remote sensing image data, applying a discriminant function for maximum likelihood classification, based on the assumption of a normal distribution representing each training class. This function is computationally expensive, since it involves two matrix multiplications for each pixel and for each class. The dimension of the matrix increases with each image band added to the classification.

The *bayes* IPW program allows for the specification of a single non-classification threshold, so that pixels whose discriminant functions for all classes that are lower than the threshold are not classified. This specified threshold parameter (-t) is a chi-square parameter and the inverse of a distance measure. Therefore, the threshold parameter had a significant effect on the proportion of the image that was classified. For example, when the threshold was set to zero, each pixel in the image was assigned to a class.

5.3 Unsupervised Classification

Clustering is a method of unsupervised image classification in which statistically similar pixels are grouped together into classes. These clusters replace the training sites used in supervised image classification. The *ustats* (IPW) program was used to generate a statistics file containing statistics for each designated cluster. The class statistics generated by *ustats* could then be used with a bayes algorithm to classify the Landsat image. This method required the determination of the input spectral bands, the desired number of output clusters, the cluster threshold radius, and which pixel value, if any, should be omitted from the clustering routine.

Firstly, the number of spectral classes for the image was decided. Following the general rule of 10 spectral classes for each land cover class in an image, the image was divided into 30 spectral classes. The advantage of obtaining a large number of spectral classes was an improved ability to distinguish differences in the spectral appearance of single land cover classes. However, the disadvantage usually involves the time-consuming

and tedious task of labeling the large number of spectral classes that are produced, since each spectral class must be identified with its informational class. Although spectral subclasses are treated as distinct units during digital classification, spectral subclasses comprising a land cover class must be labeled and subsequently displayed under a single symbol for the final image or map to be useful.

Secondly, a cluster threshold radius value (or the maximum distance from the cluster a pixel can be in spectral space and still be merged with the cluster) was selected. This value is usually determined by some trial-and-error and the process was largely a subjective operation. In general, by reducing the threshold radius, the homogeneity of the resulting clusters tended to increase, while the total number of pixels included in clusters was reduced. The larger the –r parameter, the more general the classes defined and fewer classes are typically needed. Initially, an –r value of 10 was used, however, this resulted in too little coverage in the image. As a result, larger radius parameters were tested. Finally, an –r value of 20 was judged to be adequate, resulting in less than 1 percent of the image defined as unclassified and almost all surface features in the image were included in the classification. For the purposes of this analysis, the minimization of unclassed pixels was thought to be desirable in order to produce a more informative land cover map of the Shestak test site. Therefore, the final map produced included 30 spectral classes with a threshold radius of 20.

Classes were manually labeled into the three land cover categories that had previously been used in the supervised classification and as endmembers in the SMA. The labeling process was accomplished primarily by analyzing the locations of pixels in each spectral class and determining which land cover class was most likely represented. Although some classes resulted in pixels that occurred in more than one land cover class, the pixels were simply labeled according to the class in which the majority of pixels occurred. For the most part, land cover categories were well represented in the image that was produced.

6 Results and Discussion

The study area was subset from the Landsat satellite image as shown in Figure 6. The corresponding forest stands for the test area were drawn and shown as a region map in Figure 7. As one can see, the test stand boundaries were highly irregular and stand areas were variable. A total of 73 test stands were present in the scene and the region map proved be a useful means of identifying to which test stand the pixels of the satellite image belonged. The six band Landsat black and white composite image is shown in Figure 8.

Figure 6: Landsat scene of the Shestak test area.

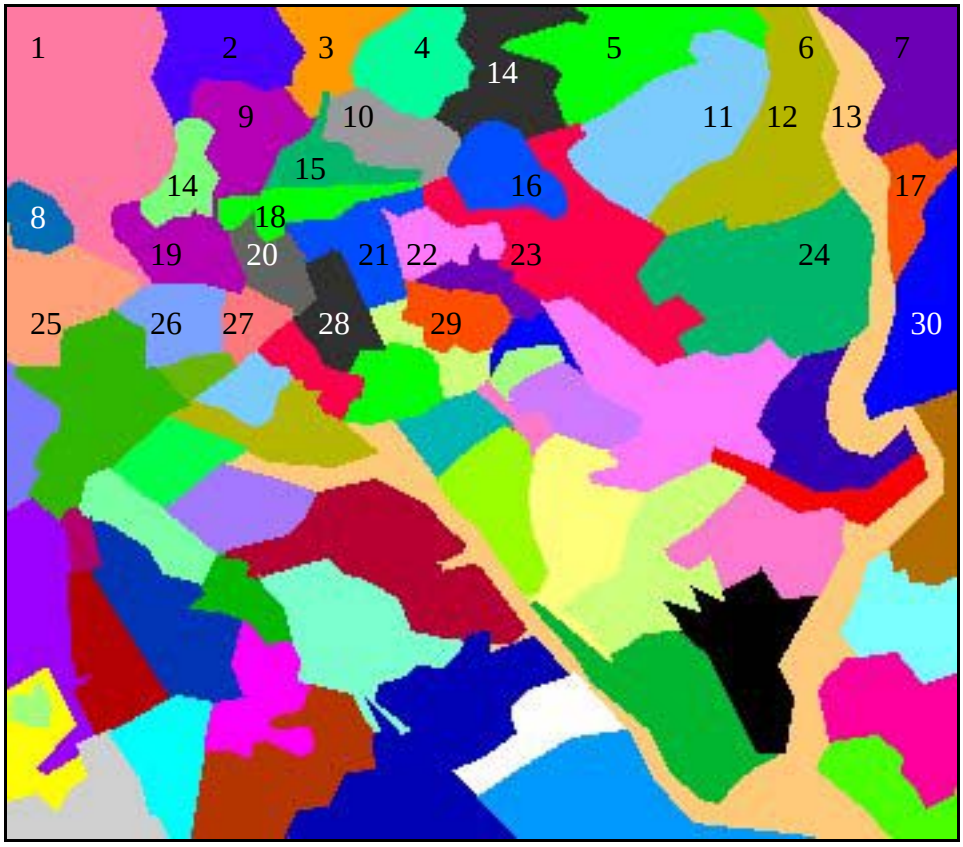

Figure 7: Region map of the subset region showing which pixels of the Landsat image belong to which respective forest test stand. A total of 73 test stands were identified in the area (stands 1 to 30 labeled).

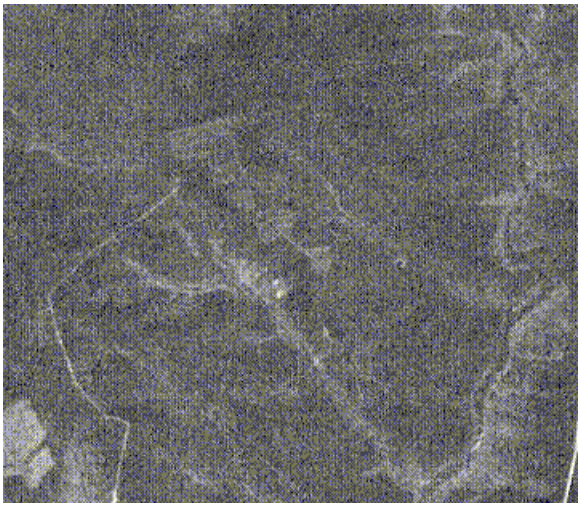

Figure 8: The six band Landsat black and white composite image.

6.1 Spectral Mixture Analysis

The primary results of interest were separate images for each of the endmembers containing an estimate of the fraction of that endmember in each pixel. Assuming the linear mixing model and that the spectral signatures of the endmembers could be derived from the training data (Table 2), the three fraction maps provided information on the abundance of the particular land cover type in each pixel of the image. The fraction maps for agriculture and floodplain soils, broadleaves, and conifers resulting from the mixture model are shown in Figures 9, 10, and 11. Digital Number (DN) values varied directly with proportional land cover; the proportions were displayed such that a DN range of 0–255 was equal to 0–100 percent (black to white). Therefore, high proportions of the endmember were indicated by higher DN or darker greytones, whereas low proportions of the endmember were indicated by lower DN or lighter greytones.

Table 2: Areal estimations of the three land cover classes from ground truth field data.

Land Cover Class	DN	Pixels	Percentage
Agriculture and Floodplain Soils	1	13933	12.56
Broadleaf Forest	2	53512	48.24
Conifer Forest	3	43484	39.20

The three individual fraction maps were combined to form a final color composite image shown in Figure 12 (Table 3). The three endmembers were matched with a color filter and identified as, (a) agriculture and floodplain soils shown in red, (b) broadleaves shown in green, and (c) conifers shown in blue. It was evident that the SMA results were beneficial in the sense that the technique recognized the fact that image pixels typically contain several different materials. "Mixed pixels" were represented by intermediate hues (i.e., orange, violet) of the endmember pure spectra and shades varied according to the proportions of each individual endmember present in each pixel. The main advantage of this technique was that target materials occupying from a whole to a small fraction of an image pixel could be detected. Therefore, the SMA provided a more accurate representation of the vegetation cover, since pixels are seldom comprised of a single land cover, but usually consist of a combination of several surface materials.

Figure 9: Fraction map for the agriculture and floodplain soils endmember (high proportion = darker tones; low proportion = lighter tones).

Figure 10: Fraction map for the broadleaf forest endmember (high proportion = darker tones; low proportion = lighter tones)..

Figure 11: Fraction map for the conifer forest endmember (high proportion = darker tones; low proportion = lighter tones).

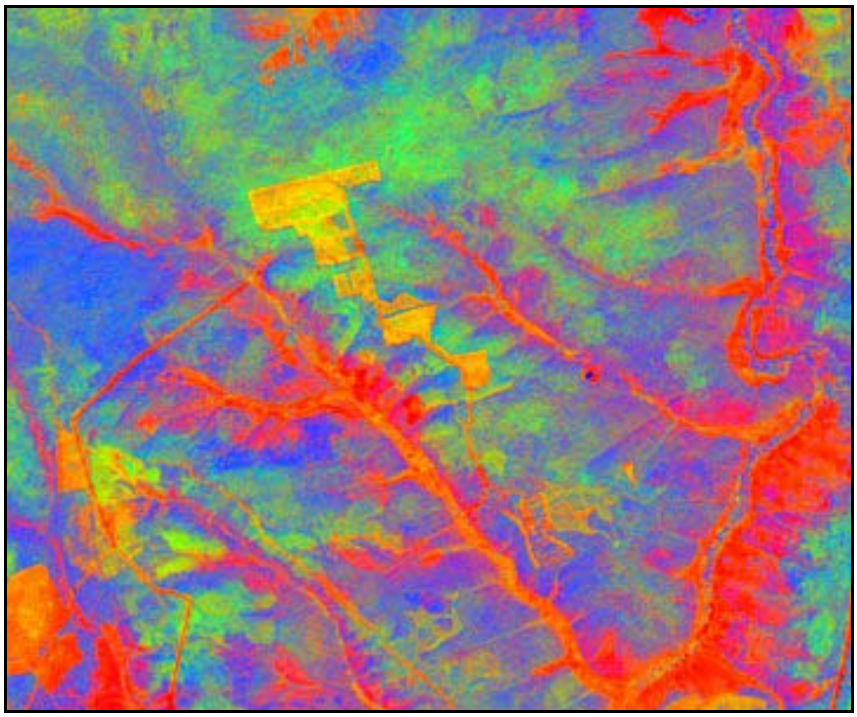

Figure 12: Color composite of the fraction maps for the three endmembers. Agriculture and floodplain soils are shown as blue, broadleaf forest as red, and conifer forest as green. Since the SMA is a subpixel classifier, each pixel is comprised of a mixture of endmember values and their corresponding color scheme. Intermediate hues represent "mixed" pixels (high proportion = darker tones; low proportion = lighter tones).

Table 3: Areal estimations of the three land cover classes from SMA.

Land Cover Class	DN	SMA Pixels	SMA Percentage	Ground Truth Percentage
Agriculture and Floodplain Soils	1	14654	13.21	12.56
Broadleaf Forest	2	55620	50.14	48.24
Conifer Forest	3	40655	36.65	39.20

A useful way of looking at the endmember values is to plot them as spectra. In Figure 13, the endmember values are plotted for each of the six Landsat bands, enabling the comparison of spectra values amongst endmembers. As expected, spectral values for each land cover type varied between image bands. However, bands 3 and 4 were particularly useful for monitoring and detecting vegetation, since these bands record in the red and near infrared spectral regions, respectively. These spectral regions are important for chlorophyll absorption, providing important indicators of plant structure, biomass, health and vigor that are useful for plant-type discrimination. Endmember values were distinct and differences were most apparent in bands 3, 4, and 5. As expected, the conifer class exhibited significantly low spectral values in bands 3 and 6, typically known to appear darker in most Landsat images. Broadleaf forest was moderate in range, but also had lowest spectral values occurring in bands 3 and 6, and highest spectral values in bands 1 and 4. In contrast, agriculture and floodplain soils appeared the brightest among the land cover classes, resulting in the highest spectral values (80–100 range) in both bands 4 and 5. Significant differences between endmember spectral values were desirable in order to distinguish among different land cover classes in the Landsat image.

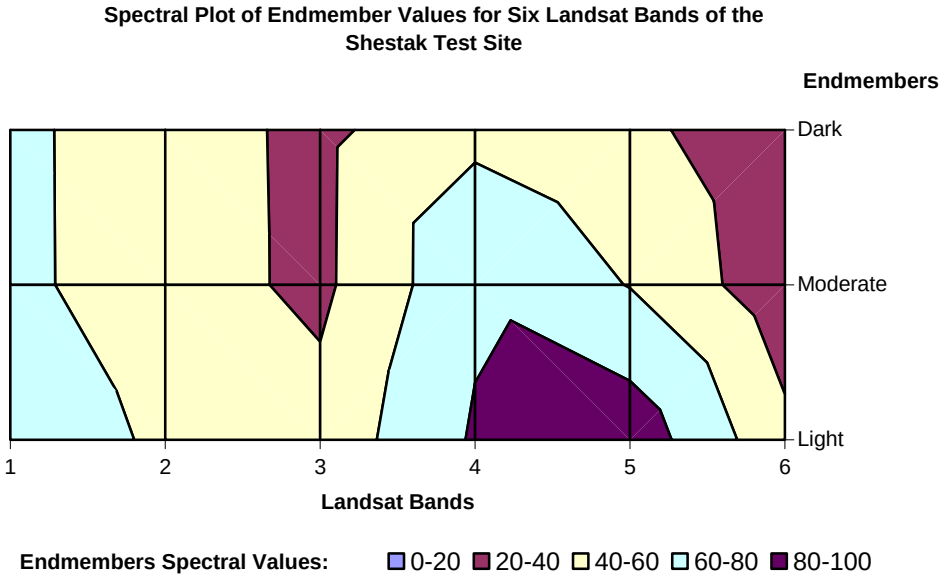

Figure 13: Spectral plot of endmember values for the six Landsat bands for the three endmembers. "Light" constitutes the agriculture and floodplain soils class, "moderate" constitutes the broadleaf forest class, and "dark" constitutes the conifer forest class. Endmember spectral values are shown according to the color scheme indicated in the legend.

6.2 Supervised Classification

The results of the supervised classification are shown in Figure 14 and the areal estimations of each land cover class are presented in Table 4. Areal estimates were relatively close to ground truth values. The three land cover and vegetation classes of agriculture and floodplain soils, broadleaves, and conifers were shown as red, green, and blue, respectively. The strategy of Maximum Likelihood classification used the training data as a means of estimating means and variances of the classes, which were then used to estimate the probabilities of all pixels belonging to the class. As a result, each pixel of the image was assigned to only one of the three discrete classification classes.

These results were generated from the IPW processing system. With respect to the threshold tolerance level, a –t value of 10 was chosen as the final threshold value. This threshold resulted in most of the image being classified and few pixels remained unclassified. Overall, this classification was judged to be adequate in terms of traditional approaches of using predefined classification schemes, since most classes occurred in areas of the scene where they were thought to actually occur. Although active vegetation classes were well defined, there were still major disadvantages associated with such hard classification schemes, as opposed to soft classification schemes offered by the SMA technique.

Although both the SMA and supervised classifier (i.e., Maximum Likelihood) used the identical training site information, the results were remarkably different and demonstrated the fundamental differences between both techniques. The SMA method was able to assess each pixel of the image individually and provide fractional estimates, thus providing more accurate areal estimates of all three land cover and vegetation type classes than those resulting from the Maximum Likelihood classifier. It is also important to note that the results of both methodologies could have been modified or further improved by editing the training data used to generate the classification results.

Table 4: Areal estimations of the three land cover classes from supervised classification.

Land Cover Class	**DN**	**Supervised Pixels**	**Supervised Percentage**	**Ground Truth Percentage**
Agriculture and Floodplain Soils	1	10222	9.13	12.56
Broadleaf Forest	2	51512	45.99	48.24
Conifer Forest	3	50274	44.88	39.20

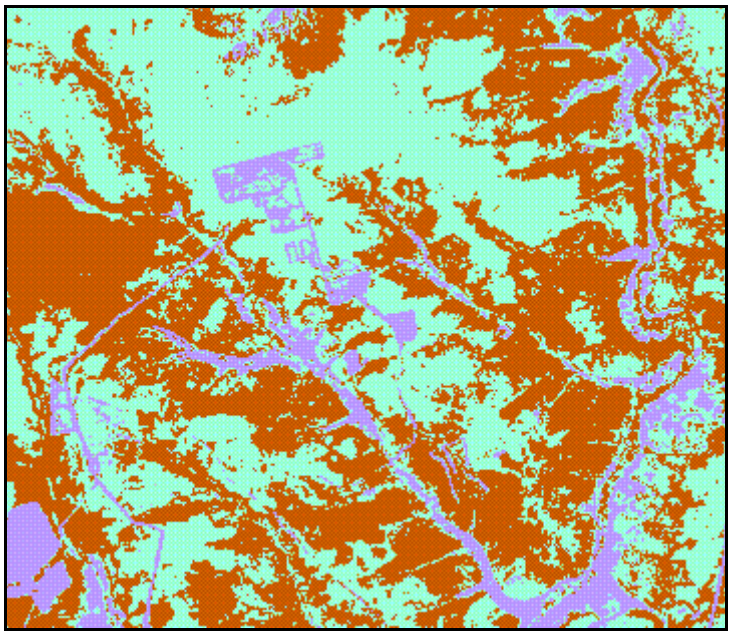

Figure 14: Classification map produced by the supervised Maximum Likelihood classifier. The agriculture and floodplain soils class is shown in violet, broadleaf forest is shown in brown, and conifer forest is shown in light green.

6.3 Unsupervised Classification

A k-means type of clustering analysis was implemented from the IPW processing system. Since threshold levels were specified to include 30 spectral classes with a threshold radius of 20, the initial map produced 30 spectral classes with relatively small clusters. Clusters were then labeled by hand into one of the three endmember classes. The final unsupervised classification image is shown in Figure 15 and areal estimates are shown in Table 5. As previously mentioned, the advantage of obtaining a large number of spectral classes was an improved ability to distinguish differences in the spectral appearance of single land cover classes. However, the trade-off exists in the difficulty in labeling the large number of spectral classes that are produced. Overall, the main difference between the supervised and unsupervised classification products was that the unsupervised classification tended to produce an image with a more "speckled" appearance. Also, the unsupervised image included unclassified pixels, whereas the supervised approach did not result with unclassified pixels, due to the high threshold parameter that was specified. In the unsupervised classification, the unclassified pixels were scattered and distributed throughout the image, especially near the boundary of most vegetation classes. The presence of unclassified pixels was an indicator of a higher level of uncertainty associated with this method of classification. Nevertheless, like the supervised approach, the unsupervised classification technique was relatively successful in generating a classification map, although it offered an "all or nothing" classification scheme and could not provide fractional estimates, unlike the SMA approach.

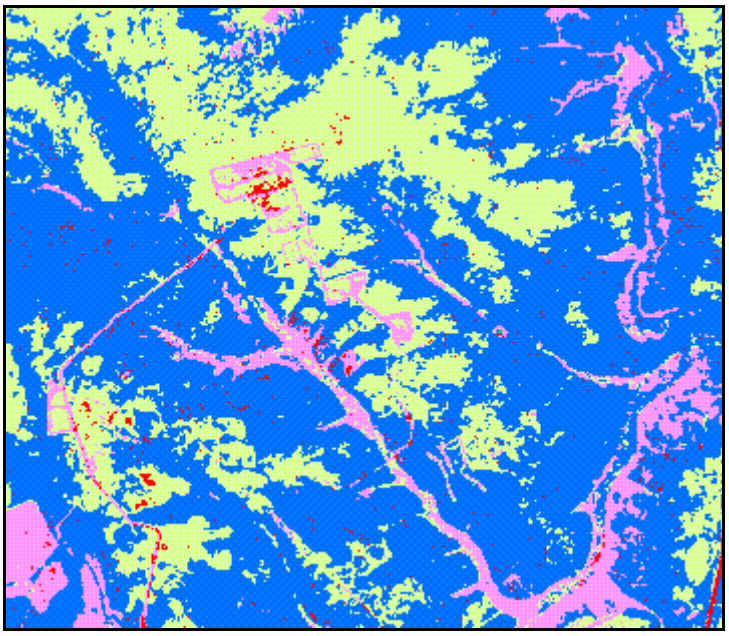

Figure 15: Classification map produced by the unsupervised classifier (using k-means cluster analysis). Agriculture and floodplain soils is shown in pink, broadleaf forest is shown in blue, and conifer forest is shown in light green. Unclassified pixels were present in the image and shown in red.

Table 5: Areal estimations of the three land cover classes from unsupervised classification.

Land Cover Class	DN	Pixels	Percentage	Ground Truth Percentage
Unclassified	0	1079	0.96	
Agriculture and Floodplain Soils	1	10256	9.16	12.56
Broadleaf Forest	2	68829	61.45	48.24
Conifer Forest	3	31844	28.43	39.20

6.4 Evaluation of Classification Methods

SMA is a physically-based image analysis process that supports repeatable and accurate extraction of quantitative subpixel information. This analysis process assumes that the spectral variability in a multispectral image can be modeled by mixtures of a small number of surface materials with distinct reflectance spectra (endmembers). In this study, the SMA was based on a linear mixing model. Unlike supervised and unsupervised image classification, the SMA did not rely on the detection or identification of pixel clusters with similar reflectance spectra. Rather, it was able to consider each pixel individually and assess the presence and proportion of select endmembers. The SMA produced fraction images that were pixel-by-pixel measures of the percent composition for each endmember in the spectral mixing model. Fraction images produced with SMA appeared to be an effective means of mapping vegetation cover and distinguishing between different vegetation and land use covers (i.e., agriculture), as well as forest tree species. The results showed that the SMA technique

was able to generate more accurate areal estimates of the endmember classes, matching closer to the field data estimates. Since supervised and unsupervised methods were based on predefined classification schemes, classifying entire pixels, this caused a "rounding-off error" to occur, often producing too high or low estimates of land cover classes due to the inability to distinguish subpixel covers. The SMA technique proved to maintain higher accuracy in classification and provided a more realistic representation of the landscape as it estimated continuous fields of land cover, as opposed to the patchy and discrete nature of traditional classification techniques.

There were several improvements that could be made to the methodology for deriving continuous fields as described in this paper. First, the training data selected to be used for estimating endmember values could be further improved. Also, the method of training data selection only indicates a discrete land cover type and not the proportion of vegetation within the training area with different vegetation characteristics. In order to truly represent proportional land cover, it should be recognized that the training sites also do not contain 100 percent pure spectra. Therefore, it must be assumed that the final values of proportional land cover were also inaccurate, since the analysis was based on inaccurate training data and erroneous assumptions for calibrating the mixture model.

Problems with assuming the linear mixture model for subpixel classification were also previously identified. Although the application of the linear mixture model offers the advantages of simplicity and ability to apply the model over large areas using existing training data, the model may also make overly simplified assumptions. For example, in linear spectral mixing, a pixel is represented by two or more surfaces that occur in patches that are large relative to the sensor's resolution and it is assumed that proportions of the components can be estimated because mixing occurs in a linear manner. However, linear mixing does not apply to cases where the composite occurs at a scale that is fine relative to the resolution of the sensor (Zhu and Evans, 1994). Since mixing would occur before radiation reaches the sensor, the components of the composite would not be able to be estimated using the linear mixing method described here. However, one should note that nonlinear mixing is likely only to occur when component surfaces arise in highly dispersed patterns. Due to the nature of the landscape and scene characteristics of the Siberian forest, the linear mixture model was judged to be adequate for the purposes of this study. However, it should be noted that other calibrated models do exist and may be more appropriate to be applied to scenes of other localities with different image characteristics.

7 Conclusion

This research investigated the use of SMA to map vegetation types of a test area in Siberia, using a portion of a single-date Landsat Enhanced Thematic Mapper (ETM) image. Results complement the findings of a small number of previous studies that support the use of SMA in mapping forest composition and areal estimates due to its ability to produce fractions representative of subpixel components directly related to forest tree type and relative area. Although the analysis used a spectral unmixing technique based on the assumptions of the linear mixture model, the mixture proportions and areal estimates that were collected corresponded well with the available

field data. This suggested that the SMA technique based on the linear mixture model was an adequate means of vegetation mapping for the purposes of this study. Furthermore, areal estimates from the SMA had higher accuracy when compared to results from traditional supervised and unsupervised classifications that used discrete classification schemes. Higher accuracy in estimating forest composition and proportional cover provides higher quality data for use in other application studies and input into ecosystem models, including carbon models or models for GHG accounting. Areas of further research could be in applying the SMA technique to other types of satellite imagery to compare results for different resolution levels. For example, data from the Moderate Resolution Imaging Spectroradiometer would provide improved spatial and spectral resolution. These data would allow refinement to the simple method described in this paper. Improvements to the SMA methodology used in this analysis could also be further explored, such as allowing for multiple endmembers, improving the determination of endmember values, and further testing and validation of the results of this study.

References

Adams, J.B., D.E. Sabol, V. Kapos, R.A. Filho, D.A. Roberts, M.O. Smith and A.R. Gillespie (1995). Classification of Multispectral Images Based on Fraction Endmembers: Application to Land-Cover Change in the Brazilian Amazon. *Remote Sensing of Environment*, 52, 137–154.

Asner, G.P., C.A. Wessman and J.L. Privette (1997). Unmixing the Directional Reflectances of AVHRR Sub-Pixel Landcovers. *IEEE Transactions on Geoscience and Remote Sensing*, 35, 868–878.

Atkinson, P.M., M.E.J. Cutler and H. Lewis (1997). Mapping Sub-Pixel Proportional Cover with AVHRR Imagery. *International Journal of Remote Sensing*, 18, 917–935.

Bateson, A. and B. Curtiss (1996). A Method for Manual Endmember Selection and Spectral Unmixing. *Remote Sensing of Environment*, 55, 229–243.

Bosdogianni, P., M. Petrou and J. Kittler (1997). Mixture Models with Higher Order Moments. IEEE *Transactions on Geoscience and Remote Sensing*, 35, 341–353.

Campbell, J.B. (1996). *Introduction to Remote Sensing*. Second Edition, The Guilford Press, New York, New York, USA.

Colwell, R.N. (1983). *Manual of Remote Sensing*. Second Edition, American Society of Photogrammetry and Remote Sensing, Falls Church, Virginia, USA.

DeFries, R.S., J.R.G. Townshend and M.C. Hansen (1999). Continuous Fields of Vegetation Characteristics at the Global Scale at 1 km Resolution. *Journal of Geophysical Research*, 104, 16911–16925.

DeFries, R.S., M.C. Hansen and J.R.G. Townshend (2000). Global Continuous Fields of Vegetation Characteristics: A Linear Mixture Model Applied to Multi-Year 8 km AVHRR Data. *International Journal of Remote Sensing*, 21, 1389–1414.

ERDAS (1997). *ERDAS Field Guide*. Fourth Edition, ERDAS Inc., Atlanta, Georgia, USA.

Foody, G. and D. Cox (1994). Sub-Pixel Land Cover Composition Estimation Using a Linear Mixture Model and Fuzzy Membership Functions. *International Journal of Remote Sensing*, 15, 619–631.

Foody, G., R.M. Lucas, P.J. Curran and M. Honzak (1997). Non-Linear Mixture Modelling Without End-Members Using An Artificial Neural Network. *International Journal of Remote Sensing*, 18, 937–953.

Jasinski, M.F. (1996). Estimation of Subpixel Vegetation Density of Natural Regions Using Satellite Multispectral Imagery. *IEEE Transactions on Geoscience and Remote Sensing*, 34, 804–813.

Moody, A. (1998). Using Landscape Spatial Relationships to Improve Estimates of Land-Cover Area From Coarse Resolution Remote Sensing. *Remote Sensing of Environment*, 64, 202–220.

Oleson, K.W., S. Sarlin, J. Garrison, S. Smith, J.L. Privette and W.J. Emergy (1995). Unmixing Multiple Land-Cover Type Reflectances from Coarse Spatial Resolution Satellite Data. *Remote Sensing of Environment*, 54, 98–112.

Quarmby, N.A., J.R.G. Townshend, J.J. Settle, M. Milnes, T.L. Hindle and N. Silleos (1992). Linear Mixture Modelling Applied to AVHRR Data for Crop Area Estimation. *International Journal of Remote Sensing*, 13, 415–425.

Roberts, D.A., M. Gardner, R. Church, S. Ustin, G. Scheer and R.O. Green (1998). Mapping Chaparral in the Santa Monica Mountains Using Multiple Endmember Spectral Mixture Models. *Remote Sensing of Environment*, 65, 267–279.

Sakhatsky, A.I., A.Y. Khodorovsky, I.J. Bujanova and I. McCallum (2002). Classification of Space Images for Forest State Identification Within the Siberia Region: Part 1. Interim Report IR-02-029. International Institute for Applied Systems Analysis, Laxenburg, Austria.

Schmullius, C., S. Voigt, S. Nilsson, T. LeToan, S. Quegan, A. Luckman, H. Balzter, W. Wagner, U. Wegmüller, W. Cramer, G. Chernjavsky, E. Vaganov, L. Vashchouk and V. Rozhkov (2002). SIBERIA II Brochure: Multi-Sensor Concepts for Greenhouse Gas Accounting in Northern Eurasia. Remote Sensing Section, Department of Geoinformatics, Friedrich-Schiller-University Jena, Germany. Available on the Internet: http://www.siberia2.uni-jena.de.

Schowengerdt, R.A. (1997). *Remote Sensing: Models and Methods for Image Processing*. Second Edition, Academic Press, New York, New York, USA.

Settle, J. and S.A. Briggs (1987). Fast Maximum Likelihood Classification of Remotely-Sensed Imagery. *International Journal of Remote Sensing*, 8, 723–734.

Settle, J. and N.A. Drake (1993). Linear Mixing and the Estimation of Ground Cover Proportions. *International Journal of Remote Sensing*, 14, 1159–1177.

Shimabukuro, Y.E. and J.A. Smith (1991). The Least-Squares Mixing Models to Generate Fraction Images Derived from Remote Sensing Multispectral Data. *IEEE Transactions on Geoscience and Remote Sensing*, 29, 16–20.

Townshend, J.R.G., C.O. Justice, D. Skole, J.P. Malingreau, J. Cihlar, P. Teillet, F. Sadowski and S. Ruttenberg (1994). The 1 km Resolution Global Data Set: Needs of the International Geosphere Biosphere Programme. *International Journal of Remote Sensing,* 15, 3417–3441.

Woodcock, C.E., J. Collins, V. Jakabhazy and S. Macomber (1993). *Technical Manual: Forest Vegetation Mapping Methods Designed for Region 5 of the U.S. Forest Service*. Boston, Massachusetts, USA.

Zhu, Z. and D.L. Evans (1994). U.S. Forest Types and Predicted Percent Forest Cover from AVHRR Data. *Photogrammetric Engineering and Remote Sensing*, 60, 525–531.